

---

# Latent Target Score Matching, with an application to Simulation-Based Inference

---

Joohwan Ko

University of Massachusetts Amherst  
johhwanko@cs.umass.edu

Tomas Geffner

NVIDIA  
tgeffner@nvidia.com

## Abstract

Denoising score matching (DSM) for training diffusion models may suffer from high variance at low noise levels. Target Score Matching (TSM) mitigates this when clean data scores are available, providing a low-variance objective. In many applications clean scores are inaccessible due to the presence of latent variables, leaving only joint signals exposed. We propose Latent Target Score Matching (LTSM), an extension of TSM to leverage joint scores for low-variance supervision of the marginal score. While LTSM is effective at low noise levels, a mixture with DSM ensures robustness across noise scales. Across simulation-based inference tasks, LTSM consistently improves variance, score accuracy, and sample quality.

## 1 Introduction

Diffusion models trained with the denoising score matching (DSM) objective [29] have emerged as a powerful class of generative models [12, 26, 27, 25, 16]. These models learn the score, the gradient of the log-density of the diffused data distribution, to parameterize a generative process for sample generation. While widely applicable [29, 26], the DSM objective may suffer from large variance as the diffusion noise level approaches zero [7], potentially degrading accuracy and sample quality. Target Score Matching (TSM) [7] addresses this, providing a low-variance training target for low noise levels in settings where clean data scores are accessible. Many problems of interest, however, involve latent variables [4]. Often, we are interested in modeling a subset of variables while treating the rest as nuisance or auxiliary components. Examples include coarse-graining in structural biology [19, 1], backbone protein design [30, 32, 14, 8], or inference tasks where only a few parameters are of interest [4]. In such cases, simulators or models may provide additional signals, such as joint density values and scores, which are unused by DSM and TSM [4, 11].

We propose Latent Target Score Matching (LTSM), a diffusion training objective tailored to models with latent variables. LTSM extends TSM by showing that the marginal score of interest (over non-latent variables) can be expressed as the conditional expectation of joint scores involving the latents. This leads to low-variance regression targets in the low-noise regime, directly addressing the shortcomings of DSM. Furthermore, LTSM can be combined with DSM through a simple time-dependent mixture, which balances accuracy near zero noise with robustness at larger noise levels. We evaluate LTSM on several simulation-based inference [28] tasks, where “gray-box” models expose joint information over parameters, latents, and observations [4]. We observe that the mixture objective that combines DSM and LTSM consistently improves over DSM in terms of score accuracy and sample quality.

## 2 Preliminaries

**Diffusion (VP-SDE).** Consider the variance preserving [27] stochastic differential equation (SDE)

$$d\theta_t = -\frac{1}{2}\beta(t)\theta_t dt + \sqrt{\beta(t)} dW_t, \quad \theta_0 \sim p_{\text{data}}(\theta), \quad (2.1)$$

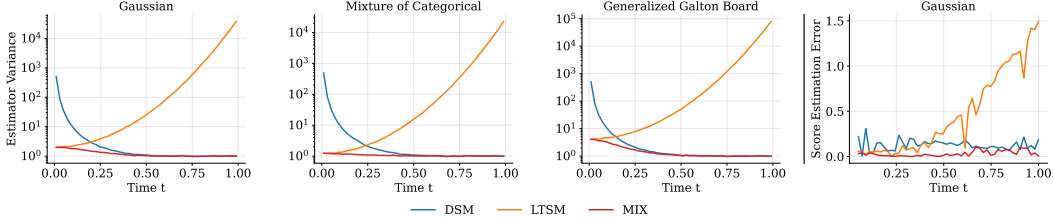


Figure 1: [Left] Regression target variance vs. diffusion time  $t$  for DSM and LTSM across three tasks (section 4). DSM rises as  $t \rightarrow 0$ , while LTSM stays low at small  $t$ , increasing for larger  $t$ . The time-dependent mixture retains the best of both methods. [Right] Score estimation error, the DSM+LTSM mixture yields the best results.

for  $t \in [0, 1]$  and  $W_t$  a standard Wiener process. Intuitively, this process gradually diffuses the data distribution towards a standard Gaussian. Given  $\theta_0$  and  $\beta(t) \geq 0$ , eq. (2.1) can be simulated exactly as  $\theta_t \sim p_t(\theta_t | \theta_0) = \mathcal{N}(\theta_t; \alpha(t)\theta_0, (1 - \alpha^2(t))I)$ , where  $\alpha(t) = \exp(-\frac{1}{2} \int_0^t \beta(s) ds)$ .

Diffusion models can be used to sample  $p_{\text{data}}(\theta)$  by simulating the time-reversal of eq. (2.1)

$$d\theta_t = [-\frac{1}{2}\beta(t)\theta_t - \beta(t)\nabla_\theta \log p_t(\theta_t)] dt + \sqrt{\beta(t)} d\bar{W}_t, \quad \theta_1 \sim N(0, I), \quad (2.2)$$

from  $t = 1$  to  $t = 0$ . This requires the score  $\nabla_\theta \log p_t(\theta_t)$ , which is typically intractable. Diffusion models approximate it using a neural network, typically trained with the DSM loss [13, 29]

$$\mathcal{L}_{\text{DSM}}(\psi) = \int_0^1 \mathbb{E}_{\theta_0, \theta_t | \theta_0} \left[ \lambda(t) \| s_\psi(\theta_t, t) - \underbrace{\nabla_{\theta_t} \log p_t(\theta_t | \theta_0)}_{y_{\text{DSM}}(\theta_0, \theta_t, t) \text{ (regression target)}} \|^2 \right] dt. \quad (2.3)$$

Since the DSM regression target  $y_{\text{DSM}}(\theta_0, \theta_t, t)$  is an unbiased estimator of the true score, i.e.,  $\nabla_{\theta_t} \log p_t(\theta_t) = \mathbb{E}_{\theta_0 | \theta_t} [\nabla_{\theta_t} \log p_t(\theta_t | \theta_0)]$ , minimizing the DSM loss trains  $s_\psi$  to approximate the true score. For the VP-SDE, the regression target from eq. 2.3 is given by  $\nabla_{\theta_t} \log p_t(\theta_t | \theta_0) = (\alpha(t)\theta_0 - \theta_t)/(1 - \alpha(t)^2)$ , with  $\alpha(t) = \exp[-1/2(\beta_{\min}t + \frac{1}{2}(\beta_{\max} - \beta_{\min})t^2)]$  for a standard linear schedule  $\beta(t) = \beta_{\min} + (\beta_{\max} - \beta_{\min})t$ . The main drawback of this estimator is its high variance as  $t \rightarrow 0$ , a problem that motivated alternative estimators with better performance for small  $t$ .

**Target Score Matching [7].** TSM is a method designed for settings where the score of the clean data  $\nabla_{\theta_0} \log p(\theta_0)$  is known. It follows the same core principle as DSM, training a network  $s_\psi$  by regressing against an unbiased estimator of the true score  $\nabla_{\theta_t} \log p_t(\theta_t)$ . The key innovation in TSM is the introduction of a different unbiased estimator, designed to have low variance as  $t \rightarrow 0$

$$\mathcal{L}_{\text{TSM}}(\psi) = \int_0^1 \mathbb{E}_{\theta_0, \theta_t | \theta_0} \left[ \lambda(t) \| s_\psi(\theta_t, t) - \underbrace{\frac{1}{\alpha(t)} \nabla_{\theta_0} \log p(\theta_0)}_{y_{\text{TSM}}(\theta_0, t) \text{ (regression target)}} \|^2 \right] dt. \quad (2.4)$$

### 3 Latent Target Score Matching

We consider a class of probabilistic models defined by a joint density  $p(\theta, z)$ , where  $\theta$  represents the variables of interest and  $z$  represents auxiliary variables, which may be latent or simply nuisance components that we do not model directly. This structure is prevalent across domains, such as structural biology (coarse-graining [19, 1], backbone protein design [30, 32, 14]), and simulation-based inference (SBI) [4], among others. Our goal is to train a diffusion model to sample the marginal  $p(\theta)$ , assuming access to samples from  $p(\theta, z)$  and the ability to evaluate the joint score  $\nabla_\theta \log p(\theta, z)$ . While DSM can be applied, as it only requires samples of  $\theta$ , it ignores the information in the joint score and may suffer from high variance as  $t \rightarrow 0$  [7]. TSM was designed to address this issue, but is not applicable, as it requires the clean marginal score  $\nabla_{\theta_0} \log p(\theta_0)$ , which is often intractable for latent-variable models. This motivates our development of Latent Target Score Matching (LTSM), a training objective that leverages the joint score to provide low-variance supervision for the marginal score. LTSM extends TSM to the latent variable setting by showing that the joint score can be used to build an unbiased estimator of the marginal score of interest:

**Proposition 3.1** (Latent Target Score Identity). *Under the VP-SDE that diffuses  $\theta$  (and not  $z$ ), we have*

$$\nabla_{\theta_t} \log p_t(\theta_t) = \frac{1}{\alpha(t)} \mathbb{E}_{\theta_0, z | \theta_t} [\nabla_{\theta_0} \log p(\theta_0, z)]. \quad (3.1)$$

This identity provides a new unbiased estimator for the marginal score of interest learned by diffusion models  $\nabla_{\theta_t} \log p_t(\theta_t)$ , which can be directly used to derive the LTSM training objective

$$\mathcal{L}_{\text{LTSM}}(\psi) = \int_0^1 \mathbb{E}_{p(\theta_0, z) p_t(\theta_t | \theta_0)} [\eta(t) \| s_\psi(\theta_t, t) - \underbrace{\frac{1}{\alpha(t)} \nabla_{\theta_0} \log p(\theta_0, z)}_{y_{\text{LTSM}}(\theta_0, z, t) \text{ (regression target)}} \|^2] dt, \quad (3.2)$$

where we denote the LTSM regression target as  $y_{\text{LTSM}}(\theta_0, z, t)$ . As intended, the LTSM target remains well-conditioned for small  $t$ , as shown in fig. 1. However, fig. 1 also shows that its variance increases for larger  $t$ , where DSM is often more stable. This complementary behavior, also noted in the original TSM work [7], motivates a new regression target obtained as an affine combination of the DSM and LTSM targets. We define the mixture regression target as

$$y_{\text{MIX}}(\theta_0, z, \theta_t, t; w_t) = w_t y_{\text{DSM}}(\theta_0, \theta_t, t) + (1 - w_t) y_{\text{LTSM}}(\theta_0, z, t), \quad (3.3)$$

where a time-dependent weight  $w_t \in \mathbb{R}$  is used to mix both targets. Since  $y_{\text{MIX}}$  is an unbiased estimator of the true score for any  $w_t$ , it can be used to obtain a new training objective

$$\mathcal{L}_{\text{MIX}}(\psi) = \int_0^1 \mathbb{E} [\eta(t) \| s_\psi(\theta_t, t) - y_{\text{MIX}}(\theta_0, z, \theta_t, t; w_t) \|^2] dt. \quad (3.4)$$

Intuitively, choosing  $w_t$  trades variance optimally across time. While its value can be chosen heuristically, we show the  $w_t$  that minimizes the variance of  $y_{\text{mix}}$  can be computed analytically:

**Proposition 3.2** (Optimal mixture weight). *Define the mixture regression target  $y_{\text{MIX}}$  as in eq. (3.3). Then, for fixed  $t$ , the weight  $w_t$  that minimizes the variance of  $y_{\text{MIX}}$  is*

$$w_t^* = \frac{\mathbb{E}[\|y_{\text{LTSM}}\|^2] - \mathbb{E}[y_{\text{DSM}}^\top y_{\text{LTSM}}]}{\mathbb{E}[\|y_{\text{DSM}}\|^2] + \mathbb{E}[\|y_{\text{LTSM}}\|^2] - 2\mathbb{E}[y_{\text{DSM}}^\top y_{\text{LTSM}}]}, \quad (3.5)$$

where expectations are w.r.t.  $(\theta_0, \theta_t, z) \sim p(\theta_0, z) p(\theta_t | \theta_0)$ . In practice, we learn  $w_t = \sigma(\text{MLP}(t))$  jointly with the score network minimizing the loss from eq. (3.4), avoiding expectation estimates.

*Proof.* We have  $w_t^* = \arg \min_{w_t} \mathbb{E}[\|y_{\text{MIX}}(w_t)\|^2]$ . Expanding  $y_{\text{MIX}}$  in terms of  $w_t$ ,  $y_{\text{DSM}}$  and  $y_{\text{LTSM}}$ , differentiating w.r.t.  $w_t$ , and setting the result to zero yields eq. (3.5).  $\square$

## 4 Experiments

We evaluate DSM (eq. (2.3)), LTSM (eq. (3.2)), and the mixture approach (eq. (3.4)) on three simulation-based inference (SBI) tasks. SBI is a powerful framework for inferring parameters  $\theta$  of complex simulators whose likelihood function  $p(x|\theta)$  is intractable. Many such simulators are "gray-box" models that rely on internal latent variables  $z$  to generate observations  $x$ , exposing a tractable joint density  $p(\theta, z, x) = p(\theta) p(z | \theta) p(x | \theta, z)$ . Given an observation  $x^*$ , the goal remains to find the posterior  $p(\theta | x^*)$  (see appendix A.1 for a detailed background). Neural SBI methods—posterior (NPE), likelihood (NLE), and diffusion-based approaches [22, 18, 5, 31, 24, 17, 9]—train amortized models on simulator-generated datasets  $\{(\theta_i, z_i, x_i)\}_{i=1}^M$ , which can be used for any  $x$  at inference time. In practice, generating large datasets by calling the simulator is often expensive. This motivates a focus on sample efficiency: achieving strong performance from a limited number of simulator calls. While diffusion models trained with DSM have proven to be a powerful approach for SBI [9], we study whether we can improve their sample efficiency by leveraging simulator's joint information via LTSM. We investigate this by training a score network  $s_\psi(\theta_t, t, x)$  to approximate  $\nabla_{\theta_t} \log p_t(\theta_t | x)$  and comparing its performance when supervised by the DSM target, the LTSM target, or their mixture.

**Simulators.** We evaluate our approach on three simulators: a Gaussian model where scores can be computed exactly, a Mixture of Categoricals, and a Generalized Galton Board [4]. We briefly describe the models here, and provide full details in appendix A.3.

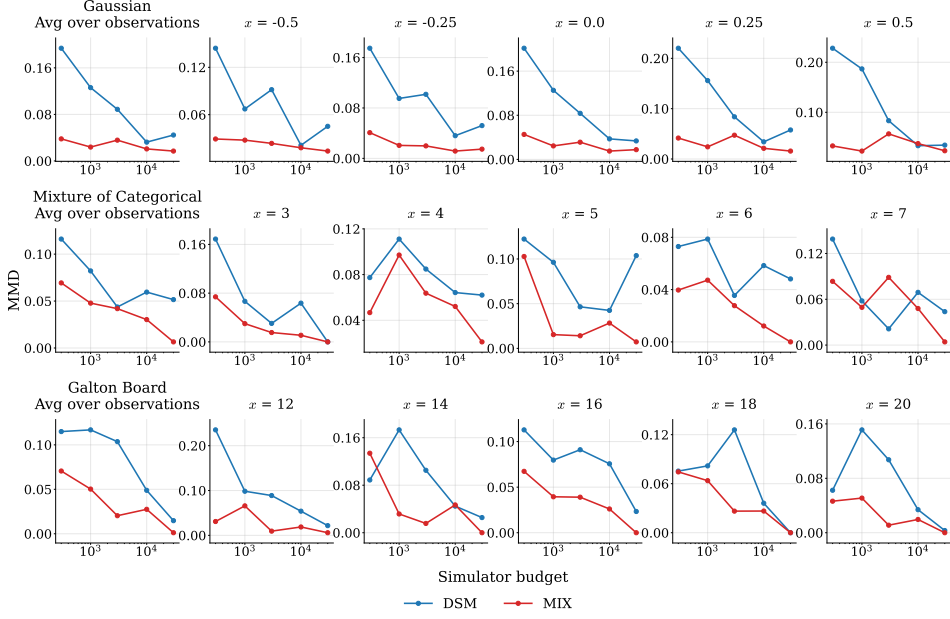


Figure 2: MMD (lower is better) vs. simulator budget (i.e. size of the dataset used for training) for each task (rows). Left column averages over five observations  $x$ ; remaining columns show results for different potential values for the observations  $x$ . The Mixture improves over DSM, with the largest gap happening for the lower number of simulator calls.

*Gaussian:*  $\theta \sim \mathcal{N}(0, 1)$ ;  $z | \theta \sim \mathcal{N}(\theta, 1)$ ;  $x | z \sim \mathcal{N}(x/3, 2/3)$ . By conjugacy  $\theta | x \sim \mathcal{N}(x/3, 2/3)$  and, diffusing only  $\theta, \theta_t | x \sim \mathcal{N}(\alpha(t)x/3, 1 - \alpha^2(t)/3)$  with  $\nabla_{\theta_t} \log p_t(\theta_t | x) = (\alpha(t)x/3 - \theta_t)/(1 - \alpha^2(t)/3)$ . These closed forms give exact error/variance curves.

*Mixture of Categorical:*  $p(\theta) = \mathcal{N}(0, 1)$ ;  $z | \theta \sim \text{Bernoulli}(\sigma(\theta))$  with  $\sigma(u) = 1/(1 + e^{-u})$ ;  $x | z \sim \text{Categorical}(\varphi^{(z)})$  over  $K$  classes,  $\varphi^{(0)} = \varphi_0, \varphi^{(1)} = \varphi_1 \in \Delta^{K-1}$ .

*Generalized Galton Board:*  $p(\theta) = \mathcal{N}(0, 1)$ ; for  $i = 1, \dots, R$  (rows),  $z_i | \theta \sim \text{Bernoulli}(\sigma(\theta))$  with logistic  $\sigma$ ; define  $s_i = 2z_i - 1$  and  $x = \text{init\_pos} + \sum_{i=1}^R s_i$  with  $\text{init\_pos} = \lfloor \text{num\_nails}/2 \rfloor$ .

**Evaluation Metrics and Setup.** To compare methods, we measure three key diagnostics in order: (1) the conditional variance of the regression target ( $y_{\text{DSM}}^x, y_{\text{LTSM}}^x, y_{\text{mix}}^x$ ) as a function of the diffusion time  $t$ ; (2) the  $\ell_1$  error between the learned score  $s_\psi(\theta_t, t, x)$  and the true score  $\nabla \log p_t(\theta_t | x)$  achieved by the different losses for the Gaussian model, where the true score can be computed analytically; and (3) the quality of the final posterior samples, assessed by the MMD [24, 10, 11] with a Gaussian kernel (appendix A.4). Unless stated otherwise, all methods share the same network architecture, noise schedule, and training budgets to ensure a fair comparison.

**Results.** Our results show a consistent trade-off across all metrics. We begin the analysis with the regression-target variance (fig. 1, left panel). As hypothesized, the DSM regression target's variance grows large as  $t \rightarrow 0$ , whereas the LTSM target remains well-conditioned at low noise levels and only grows for larger  $t$ . The mixed regression target (with the optimal weight from eq. (3.5)) leverages the best of both worlds, combining their complementary strengths to maintain low variance across all noise levels. We report both the optimal weights  $w_t^*$  and the trained  $w_t$  as functions of  $t$  in appendix A.5. This fundamental difference in variance directly translates to score estimation accuracy. On the Gaussian task, where the true score is known (fig. 1, right panel), the Mixture (MIX) objective yields the approximation with the lowest overall error, by leveraging LTSM's accuracy at small  $t$  and DSM's robustness at larger  $t$ . Ultimately, these improvements in score estimation yield higher-quality posterior samples, the main goal in SBI. As shown by the MMD results in fig. 2, the MIX method consistently generates better posterior samples than DSM across all tasks, and for several different potential observations  $x^*$ . The performance gains are most significant for smaller simulator budgets, demonstrating the improved sample efficiency of our approach.

## References

- [1] Marloes Arts, Victor Garcia Satorras, Chin-Wei Huang, Daniel Zugner, Marco Federici, Cecilia Clementi, Frank Noé, Robert Pinsler, and Rianne van den Berg. Two for one: Diffusion models and force fields for coarse-grained molecular dynamics. *Journal of Chemical Theory and Computation*, 19(18):6151–6159, 2023.
- [2] Mark A Beaumont. Approximate bayesian computation. *Annual review of statistics and its application*, 6(1):379–403, 2019.
- [3] David M Blei, Alp Kucukelbir, and Jon D McAuliffe. Variational inference: A review for statisticians. *Journal of the American statistical Association*, 112(518):859–877, 2017.
- [4] Johann Brehmer, Gilles Louppe, Juan Pavez, and Kyle Cranmer. Mining gold from implicit models to improve likelihood-free inference. *Proceedings of the National Academy of Sciences*, 117(10):5242–5249, 2020.
- [5] Jeffrey Chan, Valerio Perrone, Jeffrey Spence, Paul Jenkins, Sara Mathieson, and Yun Song. A likelihood-free inference framework for population genetic data using exchangeable neural networks. In S. Bengio, H. Wallach, H. Larochelle, K. Grauman, N. Cesa-Bianchi, and R. Garnett, editors, *Advances in Neural Information Processing Systems*, volume 31. Curran Associates, Inc., 2018.
- [6] Kyle Cranmer, Johann Brehmer, and Gilles Louppe. The frontier of simulation-based inference. *Proceedings of the National Academy of Sciences*, 117(48):30055–30062, 2020.
- [7] Valentin De Bortoli, Michael Hutchinson, Peter Wirsberger, and Arnaud Doucet. Target score matching. *arXiv preprint arXiv:2402.08667*, 2024.
- [8] Tomas Geffner, Kieran Didi, Zuobai Zhang, Danny Reidenbach, Zhonglin Cao, Jason Yim, Mario Geiger, Christian Dallago, Emine Kucukbenli, Arash Vahdat, et al. Proteina: Scaling flow-based protein structure generative models. *arXiv preprint arXiv:2503.00710*, 2025.
- [9] Tomas Geffner, George Papamakarios, and Andriy Mnih. Compositional score modeling for simulation-based inference. In *International Conference on Machine Learning*, pages 11098–11116. PMLR, 2023.
- [10] David Greenberg, Marcel Nonnenmacher, and Jakob Macke. Automatic posterior transformation for likelihood-free inference. In *International conference on machine learning*, pages 2404–2414. PMLR, 2019.
- [11] Joeri Hermans, Volodimir Begy, and Gilles Louppe. Likelihood-free MCMC with amortized approximate ratio estimators. In Hal Daumé III and Aarti Singh, editors, *Proceedings of the 37th International Conference on Machine Learning*, volume 119 of *Proceedings of Machine Learning Research*, pages 4239–4248. PMLR, 13–18 Jul 2020.
- [12] Jonathan Ho, Ajay Jain, and Pieter Abbeel. Denoising diffusion probabilistic models. *Advances in neural information processing systems*, 33:6840–6851, 2020.
- [13] Aapo Hyvärinen and Peter Dayan. Estimation of non-normalized statistical models by score matching. *Journal of Machine Learning Research*, 6(4), 2005.
- [14] John B Ingraham, Max Baranov, Zak Costello, Karl W Barber, Wujie Wang, Ahmed Ismail, Vincent Frappier, Dana M Lord, Christopher Ng-Thow-Hing, Erik R Van Vlack, et al. Illuminating protein space with a programmable generative model. *Nature*, 623(7989):1070–1078, 2023.
- [15] Michael I Jordan, Zoubin Ghahramani, Tommi S Jaakkola, and Lawrence K Saul. An introduction to variational methods for graphical models. *Machine learning*, 37(2):183–233, 1999.
- [16] Tero Karras, Miika Aittala, Timo Aila, and Samuli Laine. Elucidating the design space of diffusion-based generative models. *Advances in neural information processing systems*, 35:26565–26577, 2022.

- [17] Jan-Matthis Lueckmann, Giacomo Bassetto, Theofanis Karaletsos, and Jakob H. Macke. Likelihood-free inference with emulator networks. In Francisco Ruiz, Cheng Zhang, Dawen Liang, and Thang Bui, editors, *Proceedings of The 1st Symposium on Advances in Approximate Bayesian Inference*, volume 96 of *Proceedings of Machine Learning Research*, pages 32–53. PMLR, 02 Dec 2019.
- [18] Jan-Matthis Lueckmann, Pedro J Goncalves, Giacomo Bassetto, Kaan Öcal, Marcel Nonnenmacher, and Jakob H Macke. Flexible statistical inference for mechanistic models of neural dynamics. *Advances in neural information processing systems*, 30, 2017.
- [19] Siewert J Marrink, H Jelger Risselada, Serge Yefimov, D Peter Tieleman, and Alex H De Vries. The martini force field: coarse grained model for biomolecular simulations. *The journal of physical chemistry B*, 111(27):7812–7824, 2007.
- [20] Nicholas Metropolis, Arianna W Rosenbluth, Marshall N Rosenbluth, Augusta H Teller, and Edward Teller. Equation of state calculations by fast computing machines. *The journal of chemical physics*, 21(6):1087–1092, 1953.
- [21] Radford M Neal. Probabilistic inference using markov chain monte carlo methods. 1993.
- [22] George Papamakarios and Iain Murray. Fast  $\varepsilon$ -free inference of simulation models with bayesian conditional density estimation. *Advances in neural information processing systems*, 29, 2016.
- [23] George Papamakarios, Eric Nalisnick, Danilo Jimenez Rezende, Shakir Mohamed, and Balaji Lakshminarayanan. Normalizing flows for probabilistic modeling and inference. *Journal of Machine Learning Research*, 22(57):1–64, 2021.
- [24] George Papamakarios, David Sterratt, and Iain Murray. Sequential neural likelihood: Fast likelihood-free inference with autoregressive flows. In *The 22nd international conference on artificial intelligence and statistics*, pages 837–848. PMLR, 2019.
- [25] Jascha Sohl-Dickstein, Eric Weiss, Niru Maheswaranathan, and Surya Ganguli. Deep unsupervised learning using nonequilibrium thermodynamics. In *International conference on machine learning*, pages 2256–2265. pmlr, 2015.
- [26] Yang Song and Stefano Ermon. Generative modeling by estimating gradients of the data distribution. *Advances in neural information processing systems*, 32, 2019.
- [27] Yang Song, Jascha Sohl-Dickstein, Diederik P Kingma, Abhishek Kumar, Stefano Ermon, and Ben Poole. Score-based generative modeling through stochastic differential equations. In *International Conference on Learning Representations*, 2021.
- [28] Alvaro Tejero-Cantero, Jan Boelts, Michael Deistler, Jan-Matthis Lueckmann, Conor Durkan, Pedro J Gonçalves, David S Greenberg, and Jakob H Macke. Sbi—a toolkit for simulation-based inference. *arXiv preprint arXiv:2007.09114*, 2020.
- [29] Pascal Vincent. A connection between score matching and denoising autoencoders. *Neural computation*, 23(7):1661–1674, 2011.
- [30] Joseph L Watson, David Juergens, Nathaniel R Bennett, Brian L Trippe, Jason Yim, Helen E Eisenach, Woody Ahern, Andrew J Borst, Robert J Ragotte, Lukas F Milles, et al. De novo design of protein structure and function with rfdiffusion. *Nature*, 620(7976):1089–1100, 2023.
- [31] Simon N Wood. Statistical inference for noisy nonlinear ecological dynamic systems. *Nature*, 466(7310):1102–1104, 2010.
- [32] Kevin E Wu, Kevin K Yang, Rianne van den Berg, Sarah Alamdari, James Y Zou, Alex X Lu, and Ava P Amini. Protein structure generation via folding diffusion. *Nature communications*, 15(1):1059, 2024.

## A Experiment Details

### A.1 Simulation-based Inference

Simulation-Based Inference (SBI) [6, 2], also known as likelihood-free inference, is a class of methods for performing Bayesian inference on models where the likelihood function is intractable. In many scientific fields, mechanistic models are expressed as simulators parameterized by  $\theta$  that generate observations  $x$ . This defines an implicit likelihood  $p(x|\theta)$  which can be sampled from by running the simulator, but cannot be evaluated analytically. The goal of SBI is to estimate the posterior distribution  $p(\theta|x)$  given a real-world observation.

The intractability of the likelihood prevents the use of traditional inference algorithms like Markov Chain Monte Carlo [20, 21] or Variational Inference [15, 3], which require explicit likelihood evaluations. Neural SBI methods [22, 18, 5, 31, 24, 17, 9] overcome this by training a surrogate model (e.g., a normalizing flow [23] or a diffusion model [27]) to approximate the posterior, likelihood, or likelihood ratio, using a dataset of  $(\theta, x)$  pairs generated by the simulator.

A crucial aspect of many simulators is their reliance on internal latent variables  $z$  to produce an observation [4]. These "gray-box" simulators have a structure  $p(\theta, z, x) = p(\theta)p(z|\theta)p(x|\theta, z)$ . While the marginal likelihood  $p(x|\theta)$  remains intractable (it would require marginalizing over the latent variables  $z$ ), the full joint likelihood  $p(x, \theta, z)$  is often tractable. This is the exact setting where our proposed method, LTSM, is applicable.

A classic example is the Galton Board (see fig. 3):

- The parameters  $\theta$  define the configuration of the nails in each row.
- The latent variables  $z$  represent the stochastic path of a dropped ball, a sequence of binary left/right bounces at each nail.
- The observation  $x$  is the final bin where the ball lands.

The inference task is: given that a ball landed in bin  $x$ , what is the posterior distribution  $p(\theta|x)$ ? The likelihood  $p(x|\theta)$  is computationally expensive, as it requires summing the probabilities of all possible paths  $z$  that end in bin  $x$ . However, for any single, complete path  $z$ , the joint probability  $p(x, z, \theta)$  can be computed. LTSM is designed to exploit this accessible joint information to learn the posterior score of interest efficiently.

### A.2 DSM and LTSM for Posterior Estimation

All identities carry over when conditioning on an observation  $x$ . We train a conditional score network  $s_\psi(\theta_t, t, x)$  and keep the forward kernel  $p_t(\theta_t | \theta_0)$  unchanged. The DSM target remains

$$y_{\text{DSM}}^x(\theta_0, \theta_t, t) := \nabla_{\theta_t} \log p_t(\theta_t | \theta_0), \quad \text{with } \mathbb{E}[y_{\text{DSM}}^x | \theta_t, x] = \nabla_{\theta_t} \log p_t(\theta_t | x).$$

LTSM becomes

$$y_{\text{LTSM}}^x(\theta_0, z, t, x) := \frac{1}{\alpha(t)} \nabla_{\theta_0} \log p(\theta_0, z | x) = \frac{1}{\alpha(t)} \nabla_{\theta_0} \log p(\theta_0, z, x),$$

and satisfies  $\mathbb{E}[y_{\text{LTSM}}^x | \theta_t, x] = \nabla_{\theta_t} \log p_t(\theta_t | x)$ . Hence the mixed target is

$$y_{\text{mix}}^x(t) = (1 - w_t) y_{\text{LTSM}}^x + w_t y_{\text{DSM}}^x,$$

and the loss integrates expectations over  $(\theta_0, z, x) \sim p(\theta, z, x)$  and  $\theta_t \sim p_t(\cdot | \theta_0)$ .

### A.3 Simulator Details

All simulators follow the SBI factorization  $p(\theta, z, x) = p(\theta)p(z|\theta)p(x|z, \theta)$ . We diffuse only  $\theta$  under the VP-SDE and keep  $z, x$  fixed. For LTSM we use the joint-score target  $y_{\text{LTSM}}(\theta_0, z, t) = (1/\alpha(t)) \nabla_{\theta_0} \log p(\theta_0, z, x)$ , where the joint gradient is obtained by forming the joint log-density and backpropagating to  $\theta_0$  via autodiff.

**Gaussian.**  $\theta \sim \mathcal{N}(0, 1)$ ,  $z | \theta \sim \mathcal{N}(\theta, 1)$ ,  $x | z \sim \mathcal{N}(z, 1)$ . Conjugacy gives  $\theta | x \sim \mathcal{N}(x/3, 2/3)$ . Diffusing only  $\theta$  yields  $\theta_t | x \sim \mathcal{N}(\alpha(t)x/3, 1 - \alpha^2(t)/3)$  and the closed-form posterior score

$$\nabla_{\theta_t} \log p_t(\theta_t | x) = \frac{\alpha(t)x/3 - \theta_t}{1 - \alpha^2(t)/3}.$$

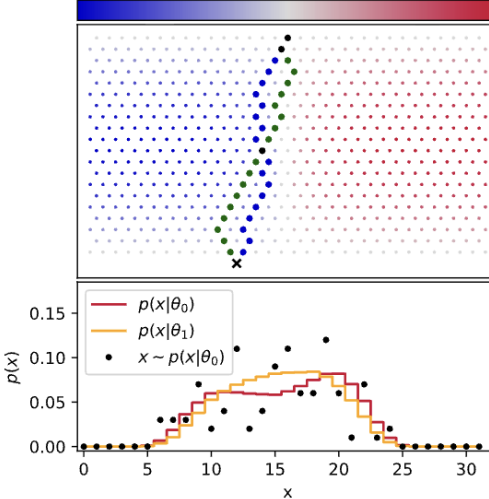


Figure 3: Toy Galton board depiction, extracted from Brehmer et al. [4]. The blue and green dark dots on the top figure represent potential paths of a ball dropped from the top. The positioning of the “nails” is defined by the parameters  $\theta$ , and the final position where the ball lands is denoted by  $x$ . For different parameters  $\theta$  the distribution of positions for the ball’s landing changes.

These closed forms are used for exact score errors and label-variance. The (analytic) joint gradient w.r.t.  $\theta$  is

$$\nabla_\theta \log p(\theta, z, x) = -\theta + (z - \theta).$$

**Mixture of Categorical.**  $p(\theta) = \mathcal{N}(0, 1)$ ;  $z \mid \theta \sim \text{Bernoulli}(\sigma(\theta))$  with  $\sigma(u) = 1/(1 + e^{-u})$ ;  $x \mid z \sim \text{Categorical}(\varphi^{(z)})$  over  $K$  classes. We instantiate  $\varphi^{(0)} = \varphi_0$  and  $\varphi^{(1)} = \varphi_1$  once by sampling logits and applying a softmax; these  $K$ -dimensional probability vectors are then held fixed. Because  $x \perp\!\!\!\perp \theta \mid z$ ,

$$\log p(\theta, z, x) = \log p(\theta) + \log p(z \mid \theta) + \log p(x \mid z) \Rightarrow \nabla_\theta \log p(\theta, z, x) = -\theta + (z - \sigma(\theta)).$$

For posterior references we use rejection sampling over simulator draws, retaining  $\theta$  when  $x$  matches a target class.

**Generalized Galton Board.**  $p(\theta) = \mathcal{N}(0, 1)$ ; for  $i = 1, \dots, R$  (number of rows),  $z_i \mid \theta \sim \text{Bernoulli}(\sigma(\theta))$  with logistic  $\sigma$ . Define steps  $s_i = 2z_i - 1 \in \{-1, +1\}$  and a deterministic readout

$$x = \text{init\_pos} + \sum_{i=1}^R s_i, \quad \text{init\_pos} = \lfloor \text{num\_nails}/2 \rfloor,$$

where `num_nails` is the number of bins/pegs across the board (so  $x \in \{0, \dots, \text{num\_nails} - 1\}$ ). Since  $x$  depends on  $z$  only, the joint gradient is

$$\nabla_\theta \log p(\theta, z, x) = -\theta + \sum_{i=1}^R (z_i - \sigma(\theta)),$$

computed via autodiff in practice. Posterior references  $p(\theta \mid x^*)$  are approximated by rejection sampling over simulator draws that hit the target bin  $x^*$ .

#### A.4 Kernel and MMD Details

**Kernel.** All distributional comparisons are performed in  $\theta$ -space ( $\theta \in \mathbb{R}^{d_\theta}$ ) using the Gaussian/RBF kernel

$$k_\sigma(u, v) = \exp\left(-\frac{\|u-v\|_2^2}{2\sigma^2}\right).$$

For each simulator and fixed observation  $x^*$ , a single bandwidth  $\sigma$  is selected once by the median-heuristic (median pairwise distance on a pilot set of reference posterior samples  $\{\theta_i \sim p(\theta \mid x^*)\}$ ) and then held fixed across methods and budgets.

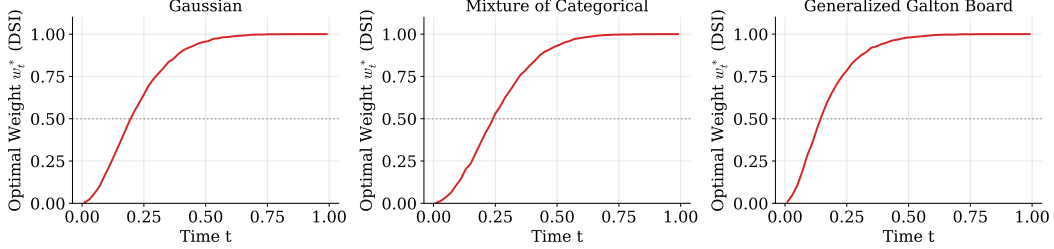


Figure 4: Variance-optimal DSM weight  $w_t^*$  vs. time  $t$ . Computed via Proposition 3.2. Here  $w_t^*$  is the coefficient on the DSM target in the mixture:  $w_t^*=0$  means pure LTSM,  $w_t^*=1$  means pure DSM. As expected,  $w_t^*$  is low near  $t \approx 0$  and increases toward 1 as  $t \rightarrow 1$ .

**Population MMD.** Given distributions  $P$  and  $Q$  on  $\mathbb{R}^{d_\theta}$ , the squared maximum mean discrepancy is

$$\text{MMD}_k^2(P, Q) = \mathbb{E}_{x, x' \sim P} k(x, x') + \mathbb{E}_{y, y' \sim Q} k(y, y') - 2\mathbb{E}_{x \sim P, y \sim Q} k(x, y),$$

which equals 0 iff  $P = Q$  for characteristic kernels such as the Gaussian.

**Estimator.** For a fixed  $x^*$ , let  $\{\theta_i\}_{i=1}^m \sim p(\theta | x^*)$  (reference) and  $\{\tilde{\theta}_j\}_{j=1}^n \sim \hat{p}(\theta | x^*)$  (model). We use the standard unbiased U-statistic

$$\widehat{\text{MMD}}_u^2 = \frac{1}{m(m-1)} \sum_{i \neq i'} k_\sigma(\theta_i, \theta_{i'}) + \frac{1}{n(n-1)} \sum_{j \neq j'} k_\sigma(\tilde{\theta}_j, \tilde{\theta}_{j'}) - \frac{2}{mn} \sum_{i=1}^m \sum_{j=1}^n k_\sigma(\theta_i, \tilde{\theta}_j),$$

and report  $\widehat{\text{MMD}} = \sqrt{\max\{\widehat{\text{MMD}}_u^2, 0\}}$ . The same kernel (and  $\sigma$ ) is used for all methods and training budgets within each task.

## A.5 Mixture Weights: Optimal vs. Learned

Recall the mixture target

$$y_{\text{mix}}^x = (1 - w_t) y_{\text{LTSM}}^x + w_t y_{\text{DSM}}^x, \quad (\text{A.1})$$

where  $w_t \in [0, 1]$  multiplies the DSM target ( $w_t=0$  = pure LTSM;  $w_t=1$  = pure DSM). proposition 3.2 gives the variance-optimal coefficient

$$w_t^* = \frac{\mathbb{E}[\|y_{\text{LTSM}}\|^2] - \mathbb{E}[y_{\text{DSM}}^\top y_{\text{LTSM}}]}{\mathbb{E}[\|y_{\text{DSM}}\|^2] + \mathbb{E}[\|y_{\text{LTSM}}\|^2] - 2\mathbb{E}[y_{\text{DSM}}^\top y_{\text{LTSM}}]}, \quad (\text{A.2})$$

with expectations over  $(\theta_0, \theta_t, z) \sim p(\theta_0, z) p_t(\theta_t | \theta_0)$  at fixed  $t$ . In fig. 4 we compute  $w_t^*$  by Monte Carlo using large simulator-generated samples at each  $t$  and clip to  $[0, 1]$ .

**Learned Weights Used In Experiments.** For all results *other than* the variance diagnostic, the mixture employs a learned schedule  $w_t$ . We parameterize  $w_t = \text{MLP}(t)$  with a sigmoid output and learn it end-to-end jointly with the score network by minimizing the standard mixture score-matching loss from section 3 (no separate variance objective). As shown in fig. 5, the learned schedules closely follow the analytic trend of  $w_t^*$ .

## B Proofs

### B.1 Standing Setting and Assumptions

We diffuse only  $\theta \in \mathbb{R}^{d_\theta}$  under the VP-SDE forward kernel

$$\theta_t = \alpha(t) \theta_0 + \sigma(t) \varepsilon_t, \quad \varepsilon_t \perp (\theta_0, z), \quad \alpha(t) > 0,$$

so that  $p_t(\theta_t | \theta_0) = q_t(\theta_t - \alpha(t)\theta_0)$  for some smooth noise density  $q_t$ . Let  $p_t(\theta_t)$  denote the marginal of  $\theta_t$  when  $(\theta_0, z) \sim p(\theta_0, z)$ .

Also, the following assumption holds for both propositions. (A1)  $p(\theta_0, z)$  and  $q_t$  are  $C^1$  in their arguments and integrable; (A2) differentiation may be interchanged with integration (dominated convergence); (A3) the integration-by-parts (IBP) boundary term in  $\theta_0$  vanishes.

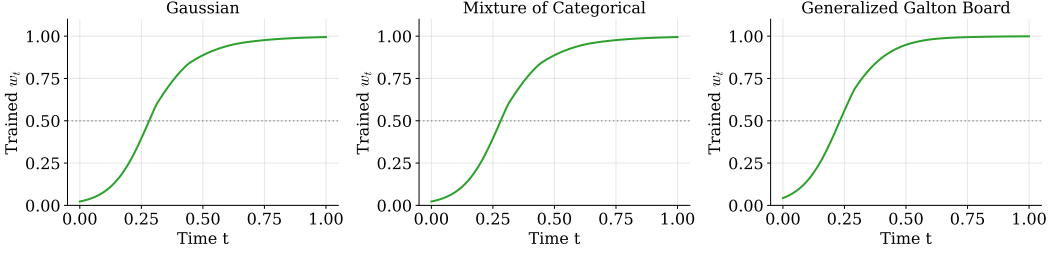


Figure 5: Learned DSM weight  $w_t$  vs. time  $t$ .  $w_t$  is the DSM coefficient in the mixture ( $0 = \text{LTSM}$ ,  $1 = \text{DSM}$ ), trained jointly with the score network. It is low near  $t \approx 0$  and rises toward 1 as  $t \rightarrow 1$ , closely tracking  $w_t^*$ .

## B.2 Latent Target Score Identity

**Proposition 3.1** (Latent Target Score Identity, LTSI). *Under the VP-SDE that diffuses  $\theta$  and keeps  $z$  fixed, the following identity holds:*

$$\nabla_{\theta_t} \log p_t(\theta_t) = \frac{1}{\alpha(t)} \mathbb{E}_{\theta_0, z | \theta_t} [\nabla_{\theta_0} \log p(\theta_0, z)]. \quad (\text{B.1})$$

*Proof.* By independence,

$$p_t(\theta_t) = \iint p(\theta_0, z) p_t(\theta_t | \theta_0) d\theta_0 dz = \iint p(\theta_0, z) q_t(\theta_t - \alpha\theta_0) d\theta_0 dz,$$

where  $\alpha = \alpha(t)$  for brevity. Differentiating inside the integral (A2),

$$\nabla_{\theta_t} p_t(\theta_t) = \iint p(\theta_0, z) \nabla_{\theta_t} q_t(\theta_t - \alpha\theta_0) d\theta_0 dz.$$

By the chain rule with  $u = \theta_t - \alpha\theta_0$ ,

$$\nabla_{\theta_t} q_t(u) = \nabla_u q_t(u) \quad \text{and} \quad \nabla_{\theta_0} q_t(u) = (-\alpha) \nabla_u q_t(u),$$

hence  $\nabla_{\theta_t} q_t(\theta_t - \alpha\theta_0) = -(1/\alpha) \nabla_{\theta_0} q_t(\theta_t - \alpha\theta_0)$ . Substitute to get

$$\nabla_{\theta_t} p_t(\theta_t) = -\frac{1}{\alpha} \iint p(\theta_0, z) \nabla_{\theta_0} q_t(\theta_t - \alpha\theta_0) d\theta_0 dz.$$

Apply vector IBP in  $\theta_0$  (A3): for each fixed  $z, \theta_t$ ,

$$\int p(\theta_0, z) \nabla_{\theta_0} q_t(\theta_t - \alpha\theta_0) d\theta_0 = [p(\theta_0, z) q_t(\theta_t - \alpha\theta_0)]_\partial - \int q_t(\theta_t - \alpha\theta_0) \nabla_{\theta_0} p(\theta_0, z) d\theta_0,$$

and the boundary term  $[ \cdot ]_\partial = 0$  by (A3). Therefore

$$\nabla_{\theta_t} p_t(\theta_t) = \frac{1}{\alpha} \iint q_t(\theta_t - \alpha\theta_0) \nabla_{\theta_0} p(\theta_0, z) d\theta_0 dz.$$

Multiply and divide by  $p_t(\theta_t)$  and also by  $p(\theta_0, z)$  inside the integral:

$$\begin{aligned} \nabla_{\theta_t} \log p_t(\theta_t) &= \frac{1}{p_t(\theta_t)} \nabla_{\theta_t} p_t(\theta_t) \\ &= \frac{1}{\alpha} \iint \underbrace{\frac{p(\theta_0, z) q_t(\theta_t - \alpha\theta_0)}{p_t(\theta_t)}}_{= p(\theta_0, z | \theta_t)} \frac{\nabla_{\theta_0} p(\theta_0, z)}{p(\theta_0, z)} d\theta_0 dz \\ &= \frac{1}{\alpha} \mathbb{E}[\nabla_{\theta_0} \log p(\theta_0, z) | \theta_t]. \end{aligned}$$

□

### B.3 Latent Target Score Matching

**Proposition B.1** (Latent Target Score Matching (LTS)). *Let  $y_{\text{LTS}}(\theta_0, z, t) := \alpha(t)^{-1} \nabla_{\theta_0} \log p(\theta_0, z)$  and  $\eta(t) > 0$ . Define*

$$\mathcal{L}_{\text{LTS}}(\psi) = \int_0^1 \eta(t) \mathbb{E}_{p(\theta_0, z) p_t(\theta_t | \theta_0)} [\|s_\psi(\theta_t, t) - y_{\text{LTS}}(\theta_0, z, t)\|^2] dt.$$

*Then, for almost every  $t \in (0, 1]$ , the unique  $L^2$  minimizer is  $s_\psi^*(\theta_t, t) = \nabla_{\theta_t} \log p_t(\theta_t)$ .*

*Proof.* Let  $y_t := \alpha(t)^{-1} \nabla_{\theta_0} \log p(\theta_0, z)$  and write the objective as

$$\mathcal{L}_{\text{LTS}}(\psi) = \int_0^1 \eta(t) \mathbb{E} [\|s_\psi(\theta_t, t) - y_t\|^2] dt, \quad \eta(t) > 0.$$

Fix  $t$  and abbreviate  $s(\cdot) := s_\psi(\cdot, t)$  and  $m(\theta_t) := \mathbb{E}[y_t | \theta_t]$ . Use the elementary identity

$$\|s(\theta_t) - y_t\|^2 = \|s(\theta_t) - m(\theta_t)\|^2 + \|y_t - m(\theta_t)\|^2 - 2\langle s(\theta_t) - m(\theta_t), y_t - m(\theta_t) \rangle.$$

Taking conditional expectation given  $\theta_t$  kills the cross term because  $\mathbb{E}[y_t - m(\theta_t) | \theta_t] = 0$ . Hence

$$\mathbb{E}[\|s(\theta_t) - y_t\|^2] = \mathbb{E}[\|s(\theta_t) - m(\theta_t)\|^2] + \mathbb{E}[\|y_t - m(\theta_t)\|^2].$$

The second term does not depend on  $s$ , and the first is minimized uniquely when  $s(\theta_t) = m(\theta_t)$  (nonnegative with equality iff  $s(\theta_t) = m(\theta_t)$  almost surely). Therefore the pointwise minimizer at time  $t$  is

$$s^*(\theta_t, t) = \mathbb{E}[y_t | \theta_t].$$

By the Latent Target Score Identity (LTSI),

$$\mathbb{E}[y_t | \theta_t] = \frac{1}{\alpha(t)} \mathbb{E}[\nabla_{\theta_0} \log p(\theta_0, z) | \theta_t] = \nabla_{\theta_t} \log p_t(\theta_t).$$

Since  $\eta(t) > 0$ , integrating over  $t$  preserves this minimizer for each  $t$ , which proves that  $s_\psi^*(\theta_t, t) = \nabla_{\theta_t} \log p_t(\theta_t)$ .  $\square$